



EUROfusion

EUROFUSION WPPFC-PR(16) 14771

T Schwarz-Selinger et al.

Deuterium retention in MeV ion implanted tungsten: influence of dose rate and damaging ion species

Preprint of Paper to be submitted for publication in
22nd International Conference on Plasma Surface Interactions
in Controlled Fusion Devices (22nd PSI)



This work has been carried out within the framework of the EUROfusion Consortium and has received funding from the Euratom research and training programme 2014-2018 under grant agreement No 633053. The views and opinions expressed herein do not necessarily reflect those of the European Commission.

This document is intended for publication in the open literature. It is made available on the clear understanding that it may not be further circulated and extracts or references may not be published prior to publication of the original when applicable, or without the consent of the Publications Officer, EUROfusion Programme Management Unit, Culham Science Centre, Abingdon, Oxon, OX14 3DB, UK or e-mail Publications.Officer@euro-fusion.org

Enquiries about Copyright and reproduction should be addressed to the Publications Officer, EUROfusion Programme Management Unit, Culham Science Centre, Abingdon, Oxon, OX14 3DB, UK or e-mail Publications.Officer@euro-fusion.org

The contents of this preprint and all other EUROfusion Preprints, Reports and Conference Papers are available to view online free at <http://www.euro-fusionscipub.org>. This site has full search facilities and e-mail alert options. In the JET specific papers the diagrams contained within the PDFs on this site are hyperlinked

Deuterium retention in MeV self-implanted tungsten: influence of damaging dose rate

T. Schwarz-Selinger

Max-Planck-Institut für Plasmaphysik, Boltzmannstr. 2, D-85748 Garching, Germany

E-mail: schwarz-selinger@ipp.mpg.de

Abstract.

Recrystallized, polycrystalline tungsten was self-damaged by 20 MeV W ions up to a calculated damage dose in the damage peak of 0.22 dpa. The time to acquire this dose and hence the average damaging dose rate was varied within three orders of magnitude from 5×10^{-3} to 4×10^{-6} dpa/sec, the latter coming close to the damage dose rate expected from fusion neutrons in future devices such as ITER and DEMO. One series was conducted at 295 K and one at 800 K to check for possible effects of defect evolution at elevated temperature. The created damage was decorated afterwards with a deuterium plasma at low ion energy of < 15 eV and low flux of 5.6×10^{19} D/m² until saturation to derive a measure for the defect density that can retain hydrogen isotopes. ³He nuclear reaction analysis (NRA) was applied to derive the deuterium depth profile and the maximum concentration in the damage peak. Neither for the 295 K nor for the 800 K series a variation in deuterium retention with damage dose rate was found. This observation supports the applicability of high rate self-ion implantation being a valid method to prepare displacement damaged tungsten as proxy material for retention studies with neutron damaged tungsten.

Keywords: tungsten, deuterium retention, displacement damage, plasma, NRA, Plasma-material interactions, ion radiation effects

29 **1. Introduction**

30

31 Taking codeposition with low-Z elements aside hydrogen isotopes retention in present-
32 day fusion devices with tungsten walls is limited by intrinsic and near-surface, plasma-
33 induced defects. In contrast, in a future thermonuclear fusion device additional trapping
34 sites will be created throughout the tungsten bulk by fast fusion neutrons which will
35 potentially increase retention by orders of magnitude. Recent experiments with fission
36 neutron irradiated tungsten show after deuterium plasma exposure deuterium
37 concentrations of up to 0.8 at.-% at 200°C [1]. However, these studies are hampered by
38 the fact that neutron exposure conditions are not well defined in terms of temperature and
39 dose rate, handling and analysis of these activated samples are typically very limited,
40 turn-around times are long, experiments are expensive, and because of that samples are
41 typically few. Systematic parameter studies are therefore not available. To overcome
42 these limitations, ions with energies of tens of keV to MeV are often used as surrogates to
43 created displacement damage. They are successfully applied in fission material
44 development for lifetime tests such as swelling since decades [2]. For fuel retention
45 studies in tungsten high energy ion implantation is used since many years and it is still a
46 field of active research [3, 4, 5, 6, 7]. Contrary to neutron irradiation, ion beam irradiation
47 is fast and does not activate the samples. However, it is still unclear in how far the
48 observations gained with this ion beam damaged surrogate material can be transferred to
49 neutron damage material. Different ions and different energies are used and it is not clear
50 which is the best to resemble the defect structure created by the collision cascades with
51 fast fusion neutrons. One parameter that was not addressed yet is the vast difference in

52 the damage creation rate between ion beam damaging and damage created by fusion
53 neutrons. There is some doubt that the biggest advantage of high energy ion implantation
54 namely its accelerated speed might create artefacts that would not be present if damage
55 creation would be conducted at the rate expected in the future fusion application. While
56 for the latter damage dose rates in the dpa range are acquired over a year they can be
57 collected within hours with an ion beam or even faster and hence damaging dose rates for
58 ion beam damaging are typically two to three orders of magnitude larger than expected
59 for future fusion devices. A prominent example for a rate dependent effect in ion beam
60 irradiation of materials is the peak swelling temperature in steels that was found to be
61 higher for higher dose rates in simple metals such as copper, nickel or stainless steel [2].
62 Hence the question arose whether this difference in damage creation rate has an effect on
63 the remaining defect structure and hence in its hydrogen isotopes retention also for
64 tungsten.

65 In this contribution the experimental setup for self-damaging is explained in detail and
66 results on the influence of the damaging dose rate on deuterium retention for tungsten
67 self-implantation will be presented.

68

69 **2. Experiment**

70

71 Hot-rolled tungsten with a purity of 99.97 wt.-%. manufactured by Plansee AG
72 (Austria) [8] was used in this study. In order to assure comparability and to minimize the
73 influence of micro-structural effects all W samples were from the same manufacturing
74 batch as in preceding studies [9, 10, 11, [12], 13, 14, [6], [7], [15]. For this study the

75 sample size was $10 \times 10 \times 0.8 \text{ mm}^3$. To allow for reliable determination of depth profiles
76 with ion beam methods the surfaces were chemo-mechanically polished to a mirror-like
77 finish following the procedure outlined in reference [10].

78 The aim of this study was to focus on the defects created by the self-damaging.
79 Therefore intrinsic defects as well as possible gaseous inclusions were minimized by re-
80 crystallizing the specimen in vacuum. First, samples were carefully outgassed and finally
81 heated to 2000 K for 2 min by electron bombardment while maintaining the pressure in
82 the low 10^{-6} Pa range. The temperature was measured with a disappearing filament
83 pyrometer during this procedure. As a consequence of the re-crystallization the
84 dislocation density is reduced by two orders of magnitude compared to the as delivered
85 state with a value of $2 \times 10^{12} \text{ m/m}^3$ [11]. The material exhibits grains with a size
86 distribution ranging from $10 \text{ }\mu\text{m}$ to $50 \text{ }\mu\text{m}$ as observed by scanning electron microscopy
87 and by confocal scanning laser microscopy. An image of a representative surface area of
88 $100 \text{ }\mu\text{m}$ by $133 \text{ }\mu\text{m}$ is shown in figure 1. Because recrystallization is performed after
89 polishing distortions from the polishing procedure are annealed out by that procedure,
90 too.

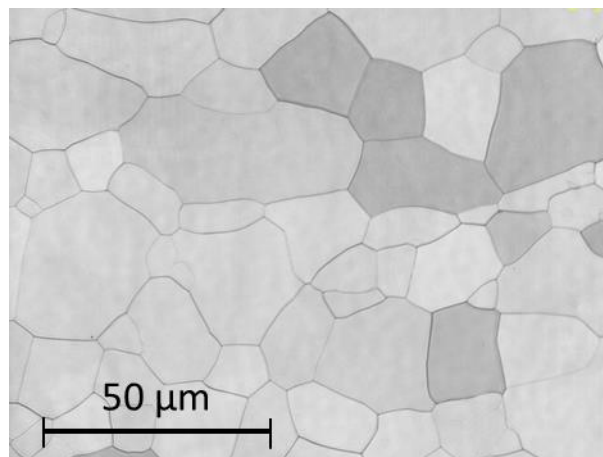


Figure 1: Confocal laser scanning microscopy image of a sample surface after polishing and annealing at 2000 K for 2 min in UHV.

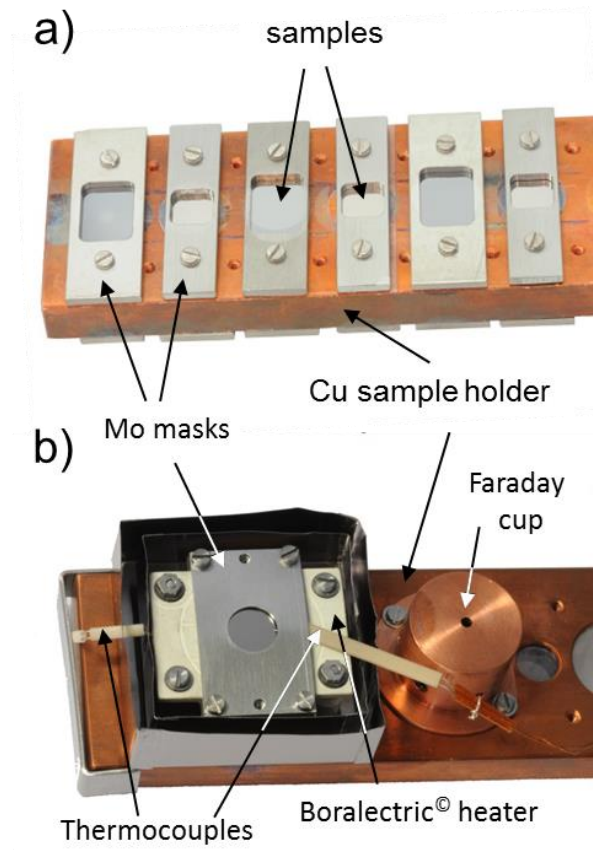


Figure 2: Sample holders for MeV tungsten implantation used in this study. a) water cooled holder with $10 \times 10 \text{ mm}^2$ samples and $12 \times 15 \text{ mm}^2$ reference samples clamped down with molybdenum masks. b) holder for implantation at elevated temperature showing the Boralectric[®] heating element, the two thermocouples, the Mo radiation shields, a sample installed with the molybdenum mask and the faraday cup for beam characterization.

91

92 Damaging was done by tungsten self-implantation with 20 MeV W^{6+} ions in the
93 TOF beamline of the 3 MV tandemron accelerator. Tungsten ions were created with a
94 caesium sputter source from a tungsten carbide target. For the first experimental series
95 samples were directly clamped down with a molybdenum mask on a water cooled copper
96 substrate holder as shown in figure 2a. The mask opening area was 9 mm x 9 mm in this

97 case. For the second series at elevated temperature samples were mounted directly on a
98 resistive heater (Boralectric[®] HTR1001) and also clamped down with a molybdenum
99 mask as shown in figure 2b. A rectangular mask with a circular opening area of 9 mm
100 was used in this case. In the present design two thermocouples are used to allow for
101 reliable temperature control of the sample. One type K thermocouple was inserted into a
102 small hole at the side of the heater itself, a second type K thermocouple was clamped
103 between the sample and the mask as shown in figure 2b. To minimize outgassing and to
104 achieve a quick response time to temperature changes the heater is mounted on a water
105 cooled support structure and surrounded by molybdenum shields as can be seen in
106 figure 2b, too. The W beam can be focused down at the target position with an
107 electrostatic quadrupole triplet lens to increase the flux density onto the target or scanned
108 over an area of up to 40 mm by 40 mm to reduce the average flux and homogenize the
109 implantation area. For the latter x- and y-deflection plates are used whose voltage supply
110 is ramped with two triangle wave-shaped crystal locked scan frequencies of close to
111 1 kHz to reach a homogenous flux throughout the implantation area. A water cooled
112 copper aperture is placed in front of the sample holder arrangement that has four faraday
113 cups in the corners and a central hole. When the beam is spread out to cross the four
114 corner cups, the absolute tungsten flux can be calculated from the measured current and
115 the cup surface areas. A central hole in the copper aperture cuts out a beam that finally
116 hits the sample. This aperture was aligned with the sample mask with an optical telescope
117 on axis. For this study arrangements with a central hole of 12 mm and 9 mm in diameter
118 were used. Figure 3 shows experimental results to characterize the beam. To measure its
119 width the beam was focused and steered into one of the four corner cups with a diameter

120 of 2 mm while manually moving the cup (red circles and left scale). In addition,
 121 deuterium retention measured with NRA of a sample implanted with 20 MeV W^{6+} with
 122 the focused beam to a fluence of $7.8 \times 10^{17} \text{ W/m}^2$ and subsequently exposed to D plasma
 123 was measured. Figure 3 shows integrated proton counts from the $D(^3\text{He},p)\alpha$ reaction
 124 measured with a ^3He energy of 2.4 MeV while scanning laterally over the sample (blue
 125 stars and the right scale). The analyzing spot width was 1 mm in that case. Both
 126 experiments show the same beam width at half maximum of 2 mm.

127 Also shown in Figure 3 are the integrated proton counts of a sample implanted
 128 with the beam spread out to homogenize the implantation (open blue square). The sample
 129 was also exposed to D plasma to decorate the defects until saturation and measured with a
 130 ^3He energy of 2.4 MeV while scanning laterally over the sample. The observed variation
 131 in D retention of 2 % is within the accuracy of the NRA analysis. We hence conclude a
 132 homogeneity of the W implantation of better than 2 %.

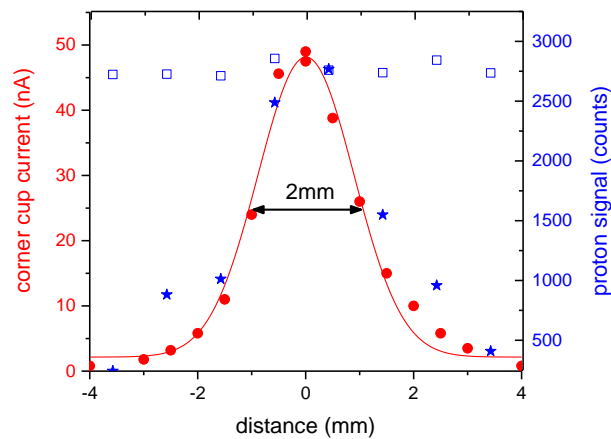


Figure 3: Beam profile measurement of the focused W beam. Red circles and left scale show the current measured in one of the four corner cups while manually moving the cup. In blue and the right scale integrated proton counts from the $D(^3\text{He},p)\alpha$ reaction are shown from a scan laterally over the sample implanted with the focused beam (blue

stars) and the scanned W beam (open squares). ^3He energy 2.4 MeV. In addition a Gaussian curve is plotted to guide the eye.

133 The current measurement from which the W flux and hence the total fluence is
134 deduced was cross checked with implanting W^{2+} with an energy of 1 MeV and a fluence
135 of $1.6 \times 10^{20} \text{ W/cm}^2$ into mirror polished pyrolytic graphite and subsequent Rutherford
136 Backscattering Spectroscopy of the implanted amount with 1 MeV protons. Comparison
137 of the measured spectra with SIMNRA simulation yields an accuracy better than 10% for
138 the absolute amount of tungsten and hence for the current measurement.

139 The measure for the damage dose is derived in this work by evaluating the
140 computed displacements from SRIM2008.04 calculations [16]. Care must be taken when
141 comparing this quantitatively to values stated in the literature. Besides obvious
142 differences when using different displacement energies (e.g. 68 eV in [5], or 90 eV in
143 [17]) subtle changes can exist using a different release of the code as well as different
144 calculation volume or number of ions. Much more serious, with the very same parameters
145 but different calculation options (“Quick Kinchin Pease” or “Full Cascade”) or evaluating
146 different output files (vacancy.txt or e2recoils.txt) there might be a difference up to a
147 factor of two depending on the procedure applied as stressed by Stoller et al. and
148 Nordlund et al. [18, 19]. These two studies recommend to use the “Quick Kinchin Pease”
149 option and it is hence used in this study. Unfortunately, all work to be found for self-
150 damage tungsten in literature till now applied the “Full cascade” option but none of them
151 state the necessary input parameters and procedures applied to allow for recalculation as
152 to convert their damage dose levels into the recommended one. In this study “dpa” values
153 are calculated using SRIM 2008.04 adding the “recoil” and “ion” displacements from the
154 “vacancy.txt” output file and converting the sum with the ion flux and the tungsten

155 density to get a depth profile of the number of displaced target atoms and the damage
156 dose in “displacements per atom”, short “dpa. Replacement collisions are neglected. A
157 displacement energy of 90 eV as recommended by American Society for Testing and
158 Materials [20] is used and a lattice binding energy of 0 eV. Although the “Quick Kinchin
159 Pease” calculation option is applied here it is compared to the “Full Cascade” calculation
160 and evaluated in the same way to be able to set it into the context of existing values in
161 literature. For this case of 20 MeV tungsten self-implantation the “vacancy.txt” output
162 yields for the “Quick Kinchin Pease” calculation 1.84 displacements per ion and
163 Ångström while it is 4.1 displacements per ion and Ångström for the “Full cascade”
164 option and hence a factor of 2.2 less. It is important to not here that this factor is not
165 unique but varies with energy.

166 Loading of the samples with deuterium was performed in the well characterized
167 low-temperature plasma experiment PlaQ [21]. To minimize the possible production of
168 additional trapping sites during deuterium loading and to decorate only the existing
169 defects without creating additional ones D exposure was performed with floating target
170 holder. At a D₂ background pressure of 1.0 Pa this results in an ion energy below 15 eV.
171 Because the ion flux consists mainly of D₃⁺ ions (94 %) with minor contributions of D₂⁺
172 (3 %) and D⁺ (3 %) I refer to this setting as <5 eV/D. For this condition the resulting D
173 flux in the form of ions is 5.6×10¹⁹ D/m²s. The flux of neutral atomic deuterium of low
174 energy (< eV) exceeds the flux of ions by at least one order of magnitude [21]. However,
175 contributions of neutral atomic deuterium are neglected here and flux refers here refer
176 here to the ion flux only. First, the implantation depth is substantially larger for the ions
177 and second the reflection coefficient is substantially smaller at higher energy so that the

178 ions should dominate retention. Recent experiments with varying bias that only influence
179 the energy of the ions supported this assumption. All samples of one series were always
180 loaded at the same time. Each sample was tightly screwed at the four corners with
181 molybdenum screws to a tungsten coated copper target holder. To avoid any defect
182 annealing or defect evolution a sample temperature of 295 K was set during D loading.
183 The time was chosen large enough to allow for D diffusion into the depth which is for the
184 given defect density and depth distribution achieved for 72 hours of exposure or a D
185 fluence of 1.5×10^{25} D/m². The temperature of the target holder was maintained by a
186 liquid cooling circuit connected to a thermostat operated with ethanol at 293 K. Sample
187 temperature was measured with a type K thermocouple spring loaded through a hole in
188 the sample holder touching the back side of one sample. In addition an IR camera was
189 used to monitor the temperature evolution as well as the lateral homogeneity of all
190 samples during the experiments.

191 Deuterium depth profiles were analysed ex-situ with the $D(^3\text{He},p)\alpha$ nuclear
192 reaction with eight different ³He energies varying from 500 keV to 4.5 MeV to probe a
193 sample depth of up to 7.4 μm. The D concentration within the near-surface layer at
194 depths of up to about 0.3 μm was determined with ³He energies of 500 keV, 690 keV and
195 800 keV by analyzing the emitted α particles with a surface barrier detector at the
196 laboratory scattering angle of 102°. A rectangular slit in front of the detector reduces the
197 solid angle to 8 msr but increases resolution. For determining the D concentration at
198 larger depths, the high energy protons were analysed using a thick, large angle solid state
199 detector at a scattering angle of 135°. A curved slit is installed in front of the detector to
200 increase resolution which reduces the solid angle to 75 msr. A nominal charge of 10 μC

201 was usually accumulated for each energy. Under 165° backscattered ^3He was detected
202 with a small surface barrier detector to accurately determine the actually acquired total
203 charge collected for each energy by simulating the spectra with SIMNRA [22]. NRADC
204 [23] was used for the deconvolution of the spectra measured at different ^3He ion energies.
205 As input data for NRADC all α and proton spectra measured at the different energies
206 were analysed simultaneously. Details about the data evaluation using NRADC can be
207 found in Ref. [22]. The present version of NRADC allows to define a depth resolution as
208 a function of depth within the Markov chain sampling. If a layer thickness below that
209 physical limit is proposed this solution is rejected. ResolNRA [24] was applied to define
210 this physical limit. For the quantitative analysis we used the cross section recently
211 published by Wielunska et al. for the protons [25] and Möller and Besenbacher for the
212 alpha particles [26]. The total amount of D retention was finally determined by
213 integrating the D profile over depth. For energy calibration purposes, to check the
214 performance of the detectors and to calibrate the solid angles of all detectors in-situ
215 amorphous, deuterated carbon thin film samples ($a\text{-C:D}$) were measured always together
216 with the samples of interest for each energy. With these precautions the accuracy of the
217 measurement can be reduced to that of the beam current measurement which is 3 %.
218 Given the counting statistics (counts depending on D content and energy) absolute
219 accuracy of the measurements reduces to the absolute accuracy of the cross section which
220 is stated as 10 % [26].

221

222 **2. Results and discussion**

223 **3.**

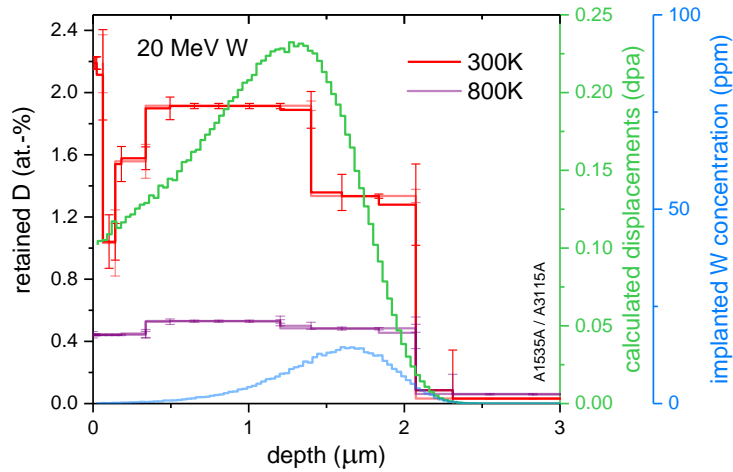
224 One possible way of changing the implantation flux and hence the damage dose
225 rate would be to use different charges states, because their abundance varies after
226 stripping the primary W⁺ beam at the terminal of the tandem accelerator. However, for a
227 fixed terminal voltage this leads to different energies of the particles and hence the
228 ambiguity introduced by the different SRIM outputs would make it complicated to
229 compare. Alternatively one could adjust the energy such that the product of charge state
230 and energy stays the same. However, one would reduce the implantation depth to well
231 below half a micron which is impractical as it is then below the depth resolution of the
232 NRA method. In addition, experiments have shown that the variation in damage dose rate
233 is limited to a factor of five.

234 Because of this uncertainty in dpa calculation and the limited accessible dynamic range
235 the W implantation energy was kept fixed at 20 MeV in the experimental series presented
236 here but the tungsten flux was varied instead. By doing this, one can directly compare the
237 experimental results as they are independent from the actual damage profile or the
238 absolute damage dose level.

239 A previous study for this material grade with 20 MeV self-implantation at room
240 temperature showed that below a value of 1.6×10^{16} W/m²s deuterium retention increases
241 linearly with damage dose, starts to deviate at higher fluences and finally saturates [15].
242 Above 7.8×10^{17} W/m²s no further increase in maximum deuterium concentration and
243 deuterium retention with damage dose is observed. This saturation regime is selected for
244 this study. Figure 3 shows the respective SRIM calculation converted into damage dose.
245 For the “Full cascade” option a peak damage dose level of 0.5 dpa is obtained for this

246 fluence, while it is 0.22 dpa for the “Quick Kinchin Pease” option as depicted in Figure 3.
247 In addition to the SRIM profile the deuterium depth profile obtained is shown in figure 3.
248 It was derived by deconvoluting the NRA data for a sample self-damaged with the
249 standard conditions comparable to those in previous publications (see [7, 14, 15]) and
250 decorated with D plasma at 295 K. Here the tungsten beam was spread out to reach the
251 four corner cups to have real time control of the implantation flux. Under these standard
252 conditions one needs an implantation time of 43 minutes to reach the intended dose of
253 7.8×10^{17} W/m²s and hence the average damage dose rate is 9.7×10^{-5} dpa_{KP}/s. Because of
254 the mention saturation with damage dose the final D depth profile is not expected to
255 follow the SRIM calculation but should be rather a flat in accordance to the experimental
256 observation. In addition, one can see that the maximum depth coincides well with the
257 depth predicted by SRIM. The error bars given in the depth profile reflect only the
258 statistical uncertainties determined by NRADC and thus do not describe the total
259 uncertainty of the measurement mentioned in the previous section. The total amount of
260 deuterium retained in the self-damaged layer is 2.3×10^{21} D/m². However, in the following
261 the value extracted from the depth profiles will be the maximum deuterium concentration
262 which is 1.9 at-% in this case as it is easier to compare to implantations at different ion
263 energies, different ions or even to neutron irradiated material.
264 As stated in the previous section the implantation flux can be reduced by spreading the
265 beam with the beam sweeping system even further. In addition the primary tungsten flux
266 can be reduced by reducing the temperature of the molybdenum ionizer in the sputter
267 source. By doing so the time to reach 0.22 dpa can be increased to 17 hours. This
268 converts to 4.2×10^{-6} dpa_{KP}/s. The obtained depth profile is identical to the one shown in

269 figure 3 within the accuracy of the method with a maximum deuterium concentration of
270 1.8 at-%. To increase the damage dose rate above the standard conditions the beam sweep
271 was switched off and the W beam was focused onto the target with the quadrupole triplet.
272 By doing this the intended W fluence can be acquired within 60 seconds which converts
273 to a dose rate of 6.3×10^{-3} dpa_{KP}/sec. Again the obtained depth profile is identical to the
274 one shown in figure 3 within the accuracy of the method. The maximum deuterium
275 concentration in this case is again 1.8 at-%. The maximum concentrations of these three
276 measurements are plotted as function of damage dose rate in figure 4. In summary,
277 variation of the damage dose rate by three orders of magnitude between 5×10^{-3} to 4×10^{-6}
278 dpa_{KP}/sec does not influence deuterium retention when damaging is conducted at room
279 temperature. Assuming a typical size of a cascade of several tens of nanometer, the given
280 damage creation rate and a typical life time of the primary damage of a few tens of
281 picoseconds this result could have been expected. However, it was not clear from the
282 beginning if longer-time scale effects play a role in damage evolution caused by
283 thermally activated processes. While vacancies are immobile at room temperature due to
284 their large migration barrier of 1.6 eV, tungsten interstitials can migrate (0.05 eV
285 migration barrier) [27]. Although these two defect types are only the easiest to consider
286 and self-damaged tungsten contains many more defect types such as vacancies clusters of
287 different size and dislocations of different geometries their energies are here only used for
288 illustration. Obviously the timescales are shorter as would be required to have any effect
289 on deuterium retention. Likewise defect evolution – such as clustering of vacancies -
290 could take place without influencing deuterium retention.



UNTITLED.epi(300K800K)
20.05.2016 22:53:14

Figure 3: Deuterium depth profile for 20 MeV self-damaged tungsten samples implanted with W^{6+} at 295 K and 800 K with an implantation fluence of $7.78 \times 10^{17} W/m^2$ and a dose rate of 10^{-4} dpa/s. D decoration was done for 72 h (1.45×10^{25} D/m²) with <5 eV/D at 295 K. In addition the damage dose (green) and the implanted tungsten concentration (blue) calculated with SRIM 2008.04 as described in the text is shown on the right axis.

291 According to Keys and Moteff annealing of defects in tungsten sets in at 0.15
 292 times the melting temperature which corresponds to 550 K [28]. Therefore the
 293 experimental sequence was repeated at a damaging temperature of 800 K. Again the
 294 damage dose rate was varied by three orders of magnitude between 5×10^{-3} and
 295 4×10^{-6} dpaKP/sec. Again the depth profile obtained for the sample prepared with
 296 “standard” conditions and decorated with D by a deuterium plasma at 295 K is show in
 297 figure 3. As expected the depth profile is again flat and reaches to the same depth for the
 298 samples damaged at room temperature. Due to defect evolution the number of traps is
 299 reduced and hence the deuterium concentration found in this sample is substantially
 300 lower. In the case of figure 3 the maximum deuterium concentration is 0.55 at-% and
 301 hence a factor of 3.5 smaller as compared to the room temperature case. It is worth
 302 mentioning that deuterium uptake for these samples damaged at 800 K is substantially
 303 larger than observed in an independent study of the same material conducted recently
 304 [29]. There the self-damaged tungsten samples implanted at 800 K were loaded with a

305 beam of atomic deuterium at 600 K and a maximum concentration of 0.14 at-% was
 306 observed. Hence thermal detrapping between D loading at 295 K and at 600 K reduces D
 307 retention by a factor of four for this type of self-damaged material.

308

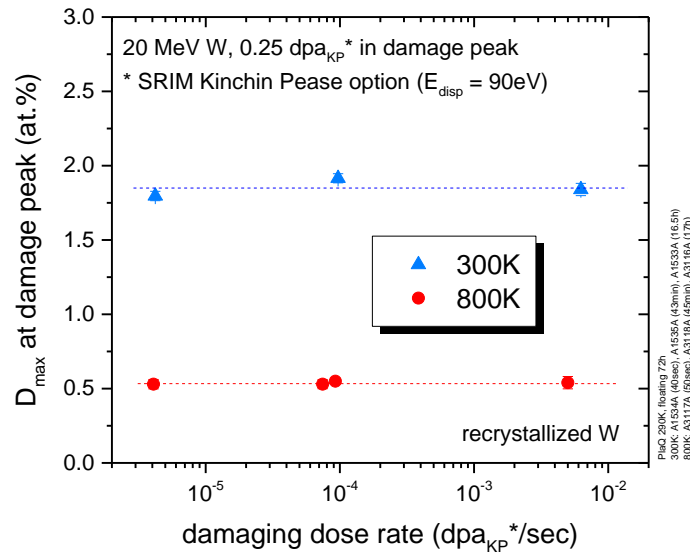


Figure 4: Maximum deuterium concentration in the self-damaged zone for recrystallized tungsten damaged with of 20 MeV W⁶⁺ at 295K and 800K as function of average damaging dose rate. D decoration was done for 72 h (1.45×10^{25} D/m²) with <5 eV/D at 295 K.

309

310 Figure four shows the maximum concentrations of this experimental series for all
 311 samples conducted in the same way as the first one except that damaging was conducted
 312 at 800 K. Also here, variation of the damage dose rate by three orders of magnitude
 313 between 5×10^{-3} to 4×10^{-6} dpa_{KP}/sec does not influence deuterium uptake. This is rather
 314 surprising given the fact that defect evolution did take place given the reduced deuterium
 315 uptake. Obvioulsy time scales in defect evolution are faster for these damage rates than
 316 would be necessary to have any effect on deuterium retention as damage evolution is

317 clearly observed by the reduced capacity of the defects at 800 K compared to the room
318 temperature case.

319 In a recent study Gilbert et al. calculated the expected damage for DEMO to be
320 smaller than 14 dpa per full power year which converts to a damage rate of around
321 4×10^{-7} dpa/sec. [30]. In a recent work by You et al. even smaller values for damage
322 creation in DEMO are mentioned which convert to damage rates of 2×10^{-7} dpa/sec [31].
323 Both values are at least an order of magnitude smaller than the damage rates accessible in
324 this experimental work. However, given the clear indication that over three orders of
325 magnitude no influence of deuterium retention is observed one can safely assume that for
326 even smaller damage dose rates no influence on D retention is expected.

327

328 **4. Conclusions**

329

330 Deuterium retention was measured in recrystallized tungsten implanted with 20 MeV
331 tungsten ions at room temperature and at 800 K for different damaging dose rates.
332 Changing the average damaging flux by three orders of magnitude between 5×10^{-3} to
333 4×10^{-6} dpa/sec does not influence D retention. Neither for the room temperature series
334 nor for the 800 K series where defect evolution clearly takes place as can be seen by the
335 reduced deuterium uptake. Obviously the time scales for defect evolution are short
336 enough to happen in between single cascade events. As damaging rates by fusion
337 neutrons in future fusion devices will be even smaller this experimental observation
338 bolster the confidence in extrapolating results derived from ion beam damaged tungsten
339 to neutron damaged tungsten.

340

341 **Acknowledgments**

342

343 I thank J. Dorner, M. Fussedler, for their help with W ion implantation and Nuclear Reaction
344 Analysis and G. Matern for polishing the samples. My colleagues at the plasma material
345 interaction group for valuable discussions. Special thanks to K. Schmid for the patience in
346 showing me how to use his NRADC code and adopting the code to my special requests.
347 Stimulating discussions with S. Markelj on D uptake in self damaged tungsten, defect annealing
348 and NRA depth profiling are greatly acknowledged.

349 Part of this work has been carried out within the framework of the EUROfusion Consortium and
350 has received funding from the Euratom research and training programme 2014-2018 under grant
351 agreement No 633053. The views and opinions expressed herein do not necessarily reflect those
352 of the European Commission.

353

354

355

356 **References**

-
- [1] M. Shimada, G. Cao, T. Otsuka, M. Hara, M. Kobayashi, Y. Oya, and Y. Hatano. "Irradiation Effect on Deuterium Behaviour in Low-Dose HFIR Neutron-Irradiated Tungsten." *Nuclear Fusion* 55, no. 1 (January 1, 2015): 13008. doi:10.1088/0029-5515/55/1/013008.
- [2] G.S. Was, *Fundamentals of Radiation Material Science: Metals and Alloys*, Springer Berlin (2010), ISBN 978-3-540-49472-0 (2010).
- [3] G.M. Wright, D.G. Whyte, B. Lipschultz. "Measurement of hydrogenic retention and release in molybdenum with the DIONISOS experiment", *J. Nucl. Mater.* 390–391 (2009) 544–549.
- [4] W.R. Wampler and R.P. Doerner, "The influence of displacement damage on deuterium retention in tungsten exposed to plasma", *Nucl. Fusion* 49, 115023 (2009), doi:10.1088/0029-5515/49/11/115023.
- [5] B. Tyburska, V.Kh. Alimov, O.V. Ogorodnikova, K. Schmid, and K. Ertl. "Deuterium Retention in Self-Damaged Tungsten." *Journal of Nuclear Materials* 395, no. 1–3 (2009): 150–55. doi:10.1016/j.jnucmat.2009.10.046.
- [6] A. Založnik, S. Markelj, T. Schwarz-Selinger, Ł. Ciupiński, J. Grzonka, P. Vavpetič, and P. Pelicon. "The Influence of the Annealing Temperature on Deuterium Retention in Self-Damaged Tungsten." *Physica Scripta T167* (2016): 14031. doi:10.1088/0031-8949/T167/1/014031.
- [7] S. Markelj, A. Založnik, T. Schwarz-Selinger, O.V. Ogorodnikova, P. Vavpetič, P. Pelicon, and I. Čadež. "In Situ NRA Study of Hydrogen Isotope Exchange in Self-Ion Damaged Tungsten Exposed to Neutral Atoms." *Journal of Nuclear Materials* 469 (2016): 133–44. doi:10.1016/j.jnucmat.2015.11.039.
- [8] PLANSEE Metall GmbH - High Performance Materials, A-6600 Reutte, Austria.
[http:// www.plansee.com](http://www.plansee.com).
- [9] A. Manhard, "Deuterium Inventory in Tungsten after Plasma Exposure: A Microstructural Survey", Ph.D. Thesis, University Augsburg, 2012.
- [10] A. Manhard, G. Matern, M. Balden: „A step-by-step analysis of the polishing process for tungsten specimens“, *Pract. Metallogr.* 50(1) , 6-15 (2013).
- [11] A. Manhard, M. Balden, S. Elgeti: „Quantitative microstructure and defect density analysis of polycrystalline tungsten reference samples after different heat treatments“, *Pract. Metallorg.* 52 (2015) 437.

-
- [12] A. Manhard, S. Kapser, L. Gao, M. Balden, S. Elgeti, T. Schwarz-Selinger, U. von Toussaint, T. Płociński, J. Grzonka, M. Gloc, Ł. Ciupiński “Microstructure and Defect Analysis in the Vicinity of Blisters in Polycrystalline Tungsten”, these proceeding.
- [13] J. Roth, T. Schwarz-Selinger, V.Kh. Alimov, and E. Markina. “Hydrogen Isotope Exchange in Tungsten: Discussion as Removal Method for Tritium.” *Journal of Nuclear Materials* 432, no. 1–3 (2013): 341–47. doi:10.1016/j.jnucmat.2012.08.004.
- [14] E. Markina, M. Mayer, A. Manhard, and T. Schwarz-Selinger. “Recovery Temperatures of Defects in Tungsten Created by Self-Implantation.” *Journal of Nuclear Materials* 463 (2015): 329–32. doi:10.1016/j.jnucmat.2014.12.005.
- [15] T. Schwarz-Selinger, W. Jacob: „Deuterium Retention in self-damaged tungsten: Saturation effects”, in preparation.
- [16] J.F. Ziegler, www.srim.org.
- [17] O.V. Ogorodnikova, B. Tyburska, V. Kh. Alimov, and K. Ertl. “The Influence of Radiation Damage on the Plasma-Induced Deuterium Retention in Self-Implanted Tungsten.” *Journal of Nuclear Materials, Proceedings of the 19th International Conference on Plasma-Surface Interactions in Controlled Fusion*, 415, no. 1, Supplement (2011): S661–66. doi:10.1016/j.jnucmat.2010.12.012.
- [18] R.E. Stoller, M. B. Toloczko, G. S. Was, A. G. Certain, S. Dwaraknath, and F. A. Garner. “On the Use of SRIM for Computing Radiation Damage Exposure.” *Nuclear Instruments and Methods in Physics Research Section B: Beam Interactions with Materials and Atoms* 310 (2013): 75–80. doi:10.1016/j.nimb.2013.05.008.
- [19] K. Nordlund, A.E. Sand, F. Granberg, S.J. Zinkle, R.E. Stoller, R.S. Averback, T. Suzudo, L. Malerba, F. Banhart, W.J. Weber, F. Willaime, S. Dudarev, D. Simeone, “Primary Radiation Damage in Materials”, Report prepared by the OECD/NEA Working Party on Multiscale Modelling of Fuels and Structural Materials for Nuclear Systems, Expert Group on Primary Radiation Damage Nuclear Science NEA/NSC/DOC(2015)9; www.oecd-nea.org
- [20] ASTM Int’l E521-96 Standard Practice for Neutron Radiation Damage Simulation by Charge-Particle Irradiation, *Annual Book of ASTM Standards vol 12.02* (Philadelphia, PA: American Society for Testing and Materials) p 7 DOI
- [21] A. Manhard, T. Schwarz-Selinger, W. Jacob, *Plasma Sources Sci. Technol.* 20 (2011) 015010.
Note: Unfortunately, the information given in the last paragraph of this article is not correct. The contribution of the molecular ions to the total ion flux for standard conditions is: $D_3^+ = 94\%$, $D_2^+ = 3\%$, and $D^+ = 3\%$. Correspondingly, the contributions to the total deuteron flux in form of ions are: 97%, 2%, and 1% as expressed correctly in figures 5 and 6 in this reference.
- [22] M. Mayer, SIMNRA User’s Guide, Report IPP 9/113, Max-Planck-Institut für Plasmaphysik, Garching, Germany, 1997 and <http://www.rzg.mpg.de/~mam/>.
- [23] K. Schmid and U. von Toussaint, *Nucl. Instr. and Meth. in Phys. Res. B* 281 64 (2012).
- [24] M. Mayer: “RESOLNRA: A New Program for Optimizing the Achievable Depth Resolution of Ion Beam Analysis Methods.” *Nuclear Instruments and Methods in Physics Research Section B: Beam Interactions with Materials and Atoms* 266, no. 8 (2008): 1852–57. doi:10.1016/j.nimb.2007.11.071.
- [25] B. Wielunska, M. Mayer, T. Schwarz-Selinger, U. von Toussaint, J. Bauer, *Nucl. Instr. Meth.* 371, 41–45 (2016).
- [26] W. Möller and F. Besenbacher, *Nucl. Instr. Meth.* 168, 111 (1980).
- [27] T. Ahlgren, K. Heinola, K. Vörtler, and J. Keinonen. “Simulation of Irradiation Induced Deuterium Trapping in Tungsten.” *Journal of Nuclear Materials* 427, no. 1–3 (2012): 152–61. doi:10.1016/j.jnucmat.2012.04.031.
- [28] L.K. Keys and J. Moteff, *Neutron Irradiation and Defect Recovery of Tungsten*, *J. Nucl. Mater.* 34 (1970).
- [29] S. Markelj, T. Schwarz-Selinger, A. Založnik, M. Kelemen, P. Vavpetič, P. Pelicon, E. Hodille, C. Grisolia, „The first study of deuterium retention in tungsten simultaneously damaged by high energy W ions and loaded by D atoms“these proceeding
- [30] Gilbert, M. R., S. L. Dudarev, D. Nguyen-Manh, S. Zheng, L. W. Packer, and J. -Ch. Sublet. “Neutron-Induced Dpa, Transmutations, Gas Production, and Helium Embrittlement of Fusion Materials.” *Journal of Nuclear Materials*, FIFTEENTH INTERNATIONAL CONFERENCE ON

FUSION REACTOR MATERIALS, 442, no. 1–3, Supplement 1 (November 2013): S755–60.

doi:10.1016/j.jnucmat.2013.03.085.

- [31] J.H. You, E. Visca, Ch. Bachmann, T. Barrett, F. Crescenzi, M. Fursdon, H. Greuner, D. Guilhem, P. Languille, M. Li, S. McIntosh, A. von Müller, J. Reiser, M. Richou, M. Rieth: „European DEMO divertor target: Operational requirements and material-design interface“, Nuclear Materials and Energy (2016)